Supporting Information

Ultra-stable Pd ions at Al T1/T2 sites on a dealuminated Pd/beta passive NOx adsorbers

Yi Zhu[a], Jun Wang[ab], Chen Wang[b,c], Jianqiang Wang[a], Gurong Shen[b,d,*], Meiqing Shen[abef,*]

[a] *Key Laboratory for Green Chemical Technology of State Education Ministry, School of Chemical Engineering & Technology, Tianjin University, Tianjin 300072, PR China*

[b] *National Rare Earth Catalysis Research Institute, Dongying 257000, PR China*

[c] *School of Environmental and Safety Engineering, North University of China, Taiyuan 030051, Shanxi, P. R. China*

[d] *Institute of New Energy Materials, School of Materials Science and Engineering, Tianjin University, Tianjin 300072, China*

[e] *State Key Laboratory of Engines, Tianjin University, Tianjin 300072, PR China*

[f] *Collaborative Innovation Center of Chemical Science and Engineering, Tianjin 300072, PR China*

1. The results of CO-DRIFTS with CO adsorption time

CO-DRIFTS was carried out on a Nicolet 6700 FT-IR spectrometer equipped with a liquid N_2 cooled mercury cadmium telluride (MCT) detector. The sample (20mg) was pressed into a self-supporting wafer with a diameter of 13mm and was inserted into a cell sealed with ZnSe windows connected with a gas manifold. The sample was oxidized in 10% O_2/N_2 for 30 min at 500 ^oC followed by cooled to 20 ^oC in N_2. Then background spectrum was obtained at 20 ^oC in N_2. After that, spectra were obtained. 1000 ppm CO/N_2 was introduced into the sample till saturation and all signals were recorded at the same time.

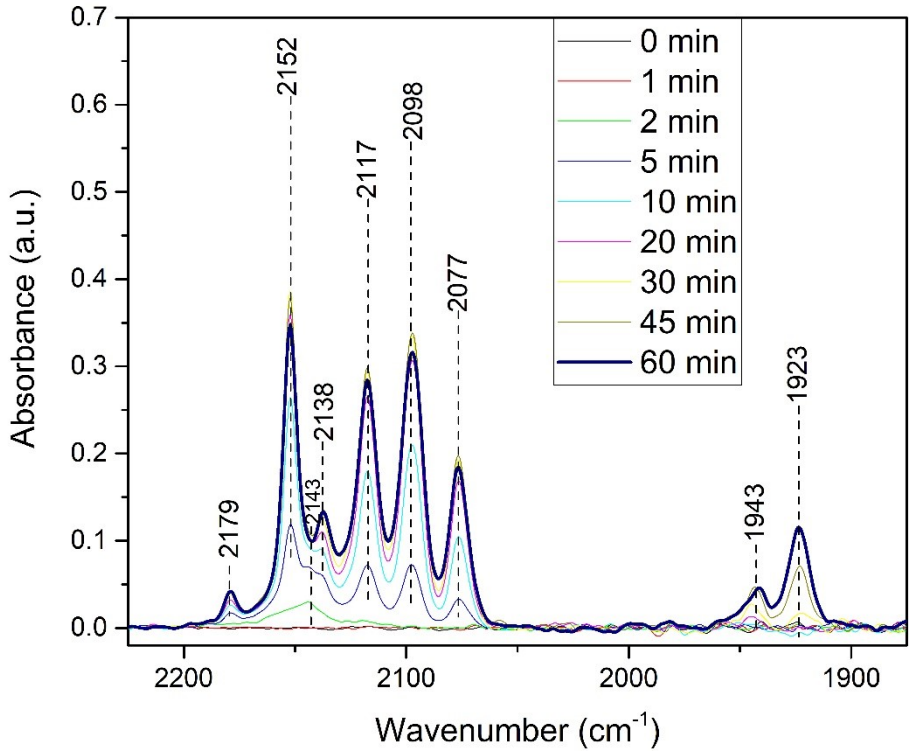

Figure S1. The CO-DRIFTS results with CO adsorption time on PB-750

2. Results of H_2-TPR on Pd/beta samples and Pd/beta-t samples

In order to investigate the effect of hydrothermal treatment and cyclic evaluations on palladium species, H_2-TPR measurements were performed on a chemisorption analyzer (Micromeritics AutoChem II 2920) coupled with a thermal conductivity detector (TCD) to accurately detect the state and content of metal oxide or ionic metal in different state. 0.25 g sample was pre-oxidized in a flow of 5% O_2/N_2 at 500 °C for 30 min prior to the measurement. After that, sample was heated from -80 °C to 900 °C at a 10 °C/min in a flow of 10% H_2/Ar. As shown in Figure S2, the aggregated Pd oxides is commonly reduced by H_2 at ca. 10 °C while the reduction of ionic Pd species is above 80 °C. The negative peak at ~70 °C is attributed to decomposition of PdH_x. And the signal of ~ -40 °C is assigned to Ar desorption.

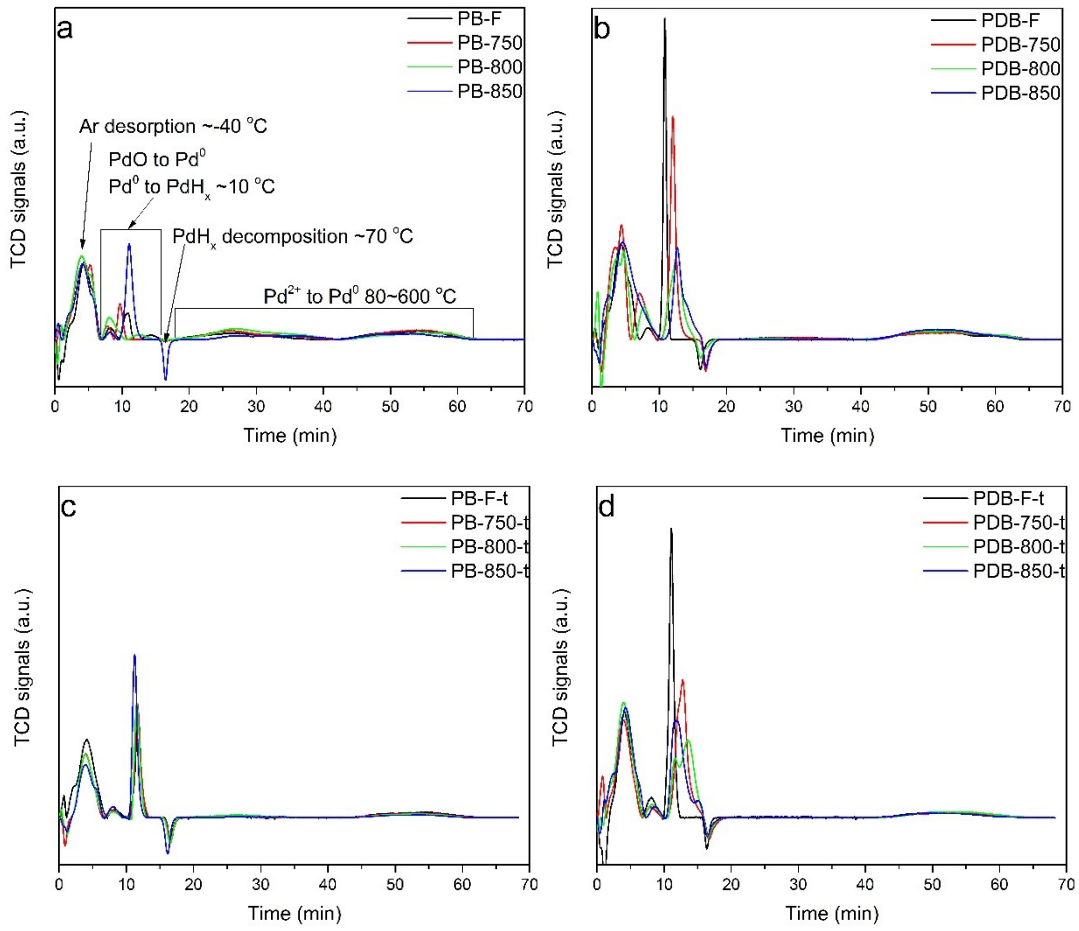

Figure S2. H_2-TPR results of (a) PB samples, (b)PDB samples, (c) PB-t samples and (d) PDB-t samples.

3. The content of Pd species by deconvoluted analysis of H_2-TPR results

In order to show the change in Pd contents affected by hydrothermal aging or cyclic evaluations, contents of various Pd species in all samples, shown in Table S1, were calculated by H_2 consumption of various peak in Figure 3 and Figure S2. Reduction of Pd species in zeolites has been proposed to occur by a one-step mechanism.[1]

$$PdO + H_2 \text{ — } Pd^0 + H_2O \quad (1)$$

$$Pd^{II} + H_2 \text{ — } Pd^0 + 2H^+ \quad (2)$$

Table S1. The content of various Pd species on all samples

Samples' Name	Content of Pd species (umol/g_{cat})						
	Total Pd	Pd oxide	Total Pd^{2+}	α	χ	δ	β
PB-F	94	16	78.0	34.2	4.2	8.9	30.7
PB-750	93.1	13.3	79.8	34.5	11.7	9.7	23.9
PB-800	94	12.3	81.7	34.1	24.3	8.6	14.7
PB-850	93	46.1	46.9	10.8	18.7	5.6	11.8
PB-F-t	93.3	54.6	38.7	5.2	0	8.5	25
PB-750-t	94	61.4	32.6	5.4	0	9.0	18.2
PB-800-t	94	63.4	30.6	8.7	0	8.2	13.7
PB-850-t	94	71.5	22.5	5.2	0	5.0	12.3
PDB-F	95	49.5	45.5	5.1	3	29.3	5.0
PDB-750	93.6	48.8	46.8	4.8	3	30.2	5.6
PDB-800	97	46.6	50.4	6.0	0.0	38.6	5.8
PDB-850	95	52.6	42.4	0.0	0.0	37.1	5.3
PDB-F-t	92	52.3	39.7	5	0	29.3	5.4
PDB-750-t	92	53	39	4.1	0	30.2	4.7
PDB-800-t	92	51.6	40.4	0	0	37.1	3.3
PDB-850-t	94	60	34	0	0	30.7	3.3

4. The NO_x adsorption and desorption curves of all samples in cyclic evaluations

Figure S3 shows the NO_x adsorption and desorption curves of all samples. The desorption signals of PB samples significantly weakens during cyclic evaluations, but is basically stable on PDB samples. The desorption temperature of PB-F's aged samples is lower than PB-F. The similar situation happens on PDB samples. This may be attributed to the change in relative crystallinity and micropore properties.

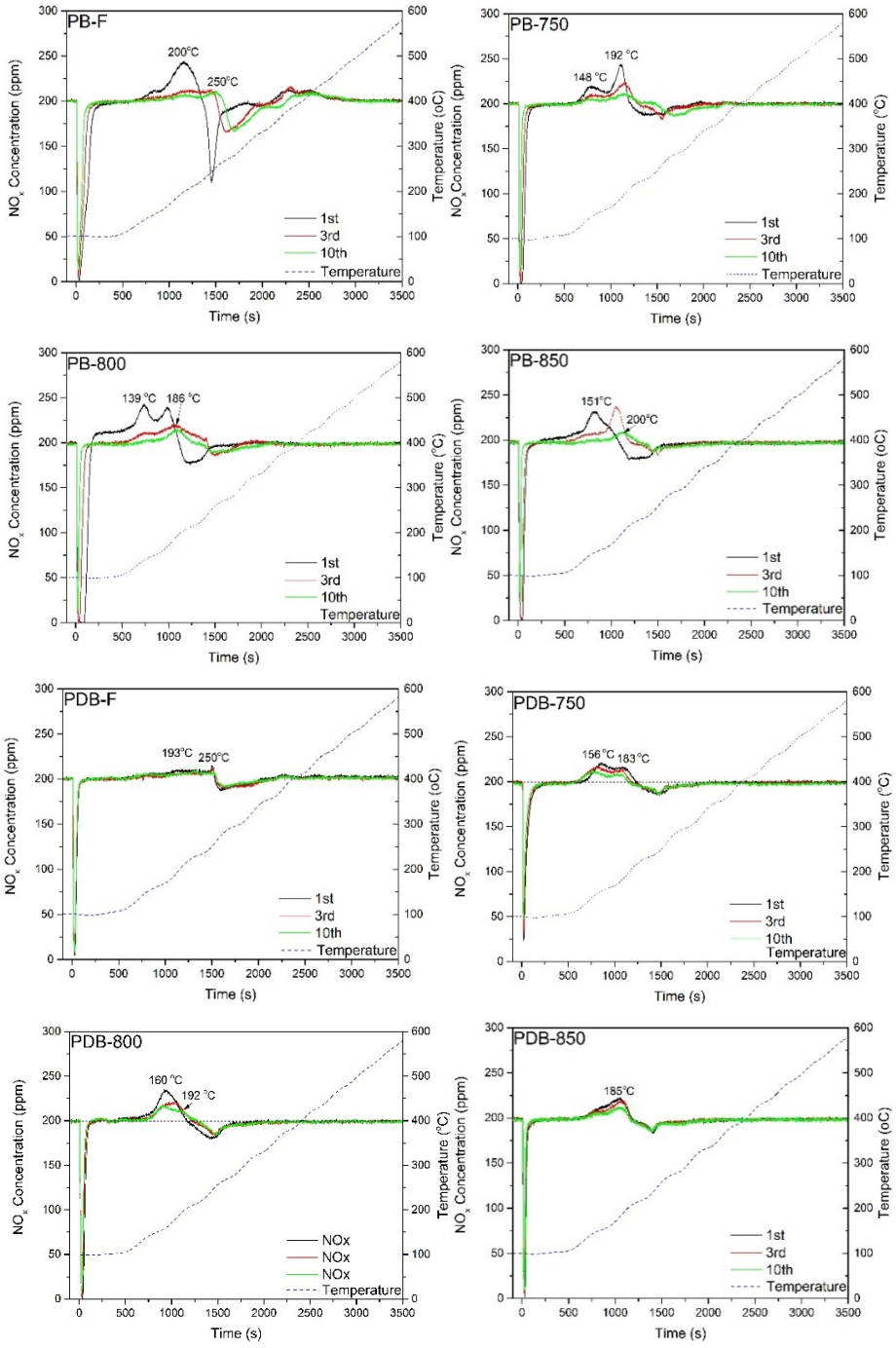

Figure S3. The NO_x adsorption and desorption curves of 1st, 3rd and 10th cycle on Pd/beta samples.

5. The effect of cyclic evaluations on crystal properties of Pd/beta samples

The X-ray diffraction (XRD) spectra were collected using a Bruker D8 Advance TXS operating at 40 kV and 40 mA with nickel-filtered Cu Ka radiation (k = 1.5418 Å). The data were collected with a step size of 0.01° in the range from 5° to 50°. In order to investigated the effect of cyclic evaluations on crystal properties of Pd/beta samples, the XRD spectra and relative crystallinity of Pd/beta samples are compared with that of Pd/beta-t samples, shown in Figure S4.

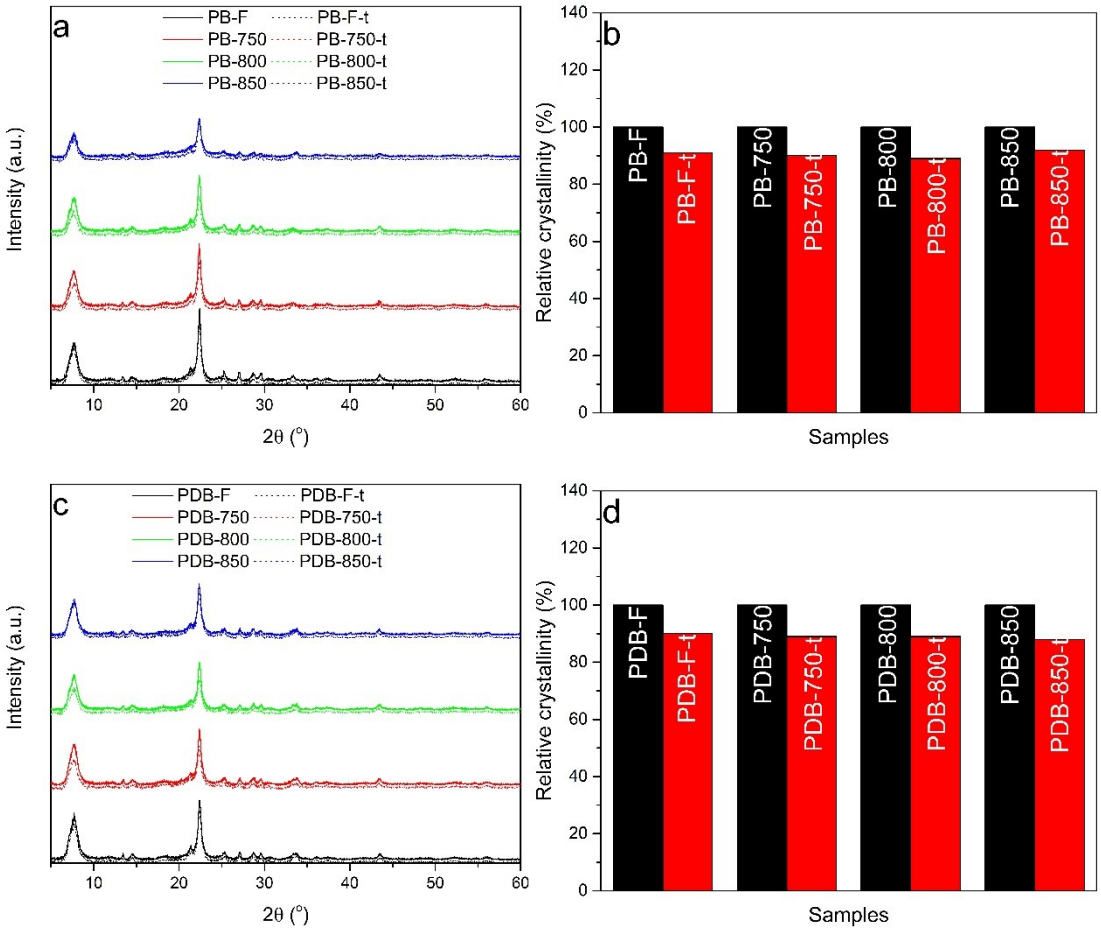

Figure S4. The XRD results of samples before and after active cyclic tests

6. The effect of cyclic evaluations on surface area and pore volume of Pd/beta samples

N_2 physical adsorption was performed with a sorption analyzer (ASAP 2460 Micromeritics Instrument Co., Norcross, GA, USA) to characterize the porous properties of samples. Samples were pre-degassed at 300 ^oC for 5 hours. The specific surface area (S_{BET}) of samples were calculated by the Burner-Emmet-Teller (BET) method and the micropore volume was calculated by DFT method. In order to investigated the effect of cyclic evaluations on pore properties of Pd/beta samples, the surface area and pore volume of Pd/beta samples are compared with that of Pd/beta-t samples, shown in Table S2.

Table S2. The physical properties of Pd/beta samples

Samples' name	Suface area m^2/g	Pore volume cm^3/g	Samples' name	Suface area m^2/g	Pore volume cm^3/g
PB-F	761	0.219	PDB-F	817	0.229
PB-F-t	679	0.195	PDB-F-t	768	0.218
PB-750	629	0.183	PDB-750	678	0.189
PB-750-t	622	0.177	PDB-750-t	674	0.186
PB-800	614	0.171	PDB-800	666	0.189
PB-800-t	585	0.17	PDB-800-t	663	0.183
PB-850	469	0.14	PDB-850	599	0.169
PB-850-t	474	0.135	PDB-850-t	619	0.175

7. The effect of hydrothermal aging on porous structure of H/beta and Pd/beta samples

Figure S5 shows the change in micropore distribution and mesopores/macropores distribution of H/beta samples and Pd/beta samples with hydrothermal temperature. Overall, the hydrothermal aging causes the micropore destroyed, and transformed into mesopores or macropores.

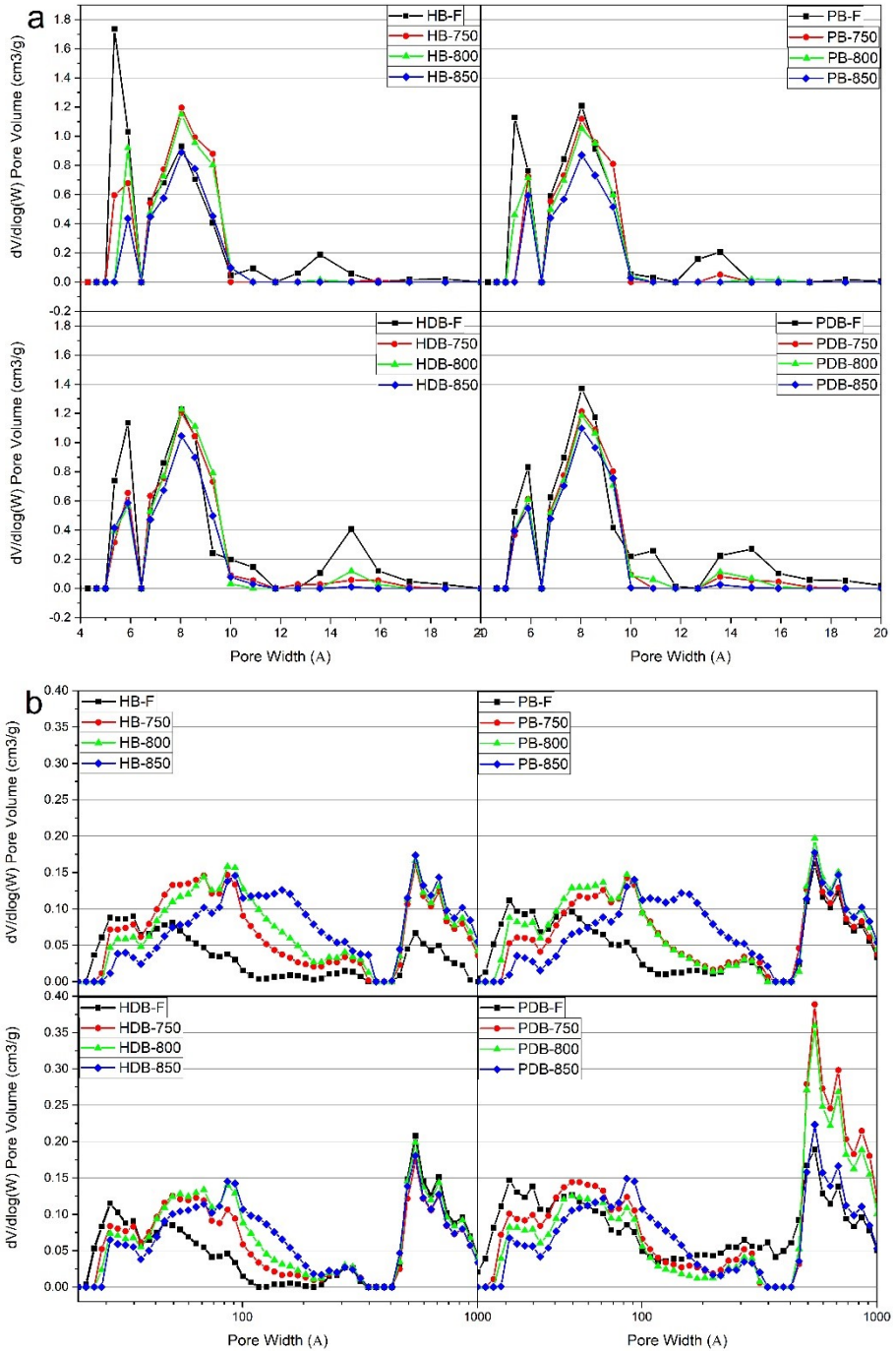

Figure S5. The (a) micropore distribution and (b) mesopores/macropores distribution of H/beta samples and Pd/beta samples

8. The effect of cyclic evaluations on acid amount by NH_3-TPD

In order to analyze the effect of cyclic evaluations on acid amount, the NH_3-TPD results of Pd/beta samples are compared with Pd/beta-t samples. Except for PB-F and PB-F-t, Pd/beta samples show a reduction of peaks A/B/C compared to corresponding Pd/beta-t. This is attributed to loss of palladium ions combined with H_2-TPR results. For PB-F and PB-F-t, the loss of peak D means the loss of Si-OH-Al species during cyclic evaluations. Because the evaluation condition is up to 600 °C and with 10% H_2O, part of unstable Si-OH-Al (Brønsted acid) is destroyed. Overall, the loss of peaks A/B/C is more severe on PB samples than that on PDB samples during cyclic evaluations.

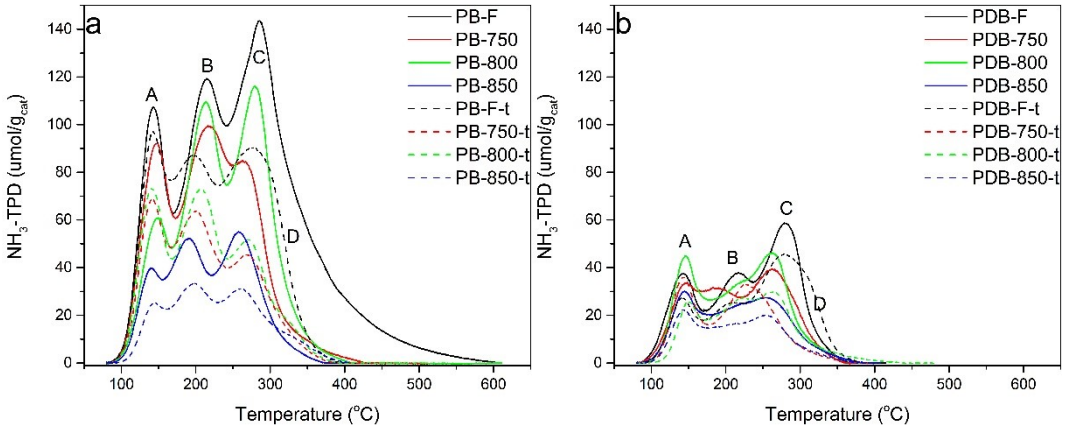

Figure S6. The NH_3-TPD results of (a) PB samples and PB-t samples; (b) PDB samples and PDB-t samples.

9. The assignment of acid species on H/beta samples

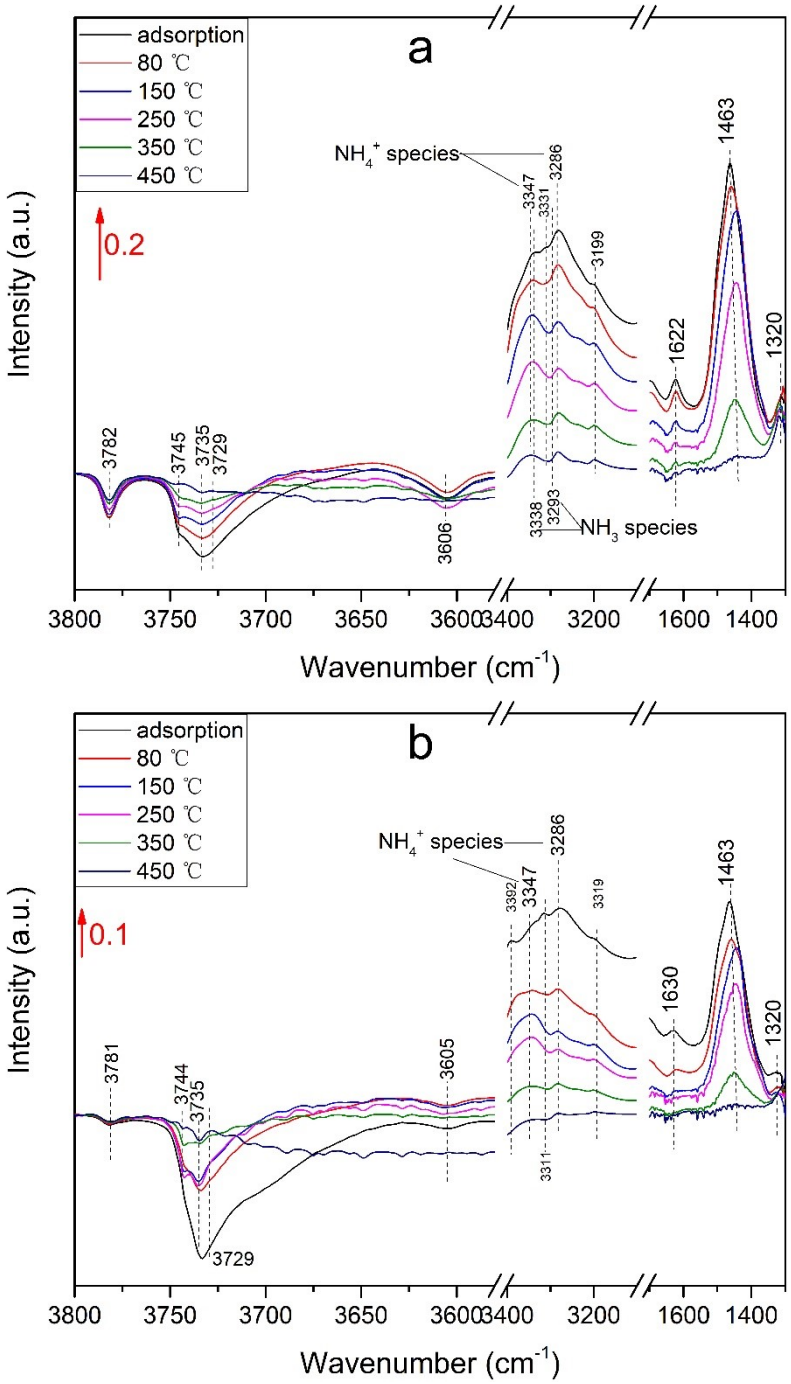

Figure S7. NH_3-IR spectra of adsorption (black line) and TPD at different temperature (red, blue, pink, green, navy line from low to high temperature) on (a) HB-F, (b) HDB-F.

The NH_3 adsorption and desorption spectra is carried out to ensure the acidity and desorption temperature of NH_3 on Beta zeolite. Assignments, based on literature, for acid sites and NH_3 adsorption species can be found in Table S3. [2-5] It's need to note that a different scale, 0.2 for HB-F and 0.1 for HDB-F is caused by the difference of signal intensity. This points out the reduction of acid content

with Si/Al ratio increasing, shown in the region from 1700 to 1300 cm^{-1}. Some negative peaks above 3000 cm^{-1} is due to NH_3 adsorbed on hydroxyl species. For H/beta, NH_3 is firstly desorbed on Si-OH species, 80 ~ 150 ^oC at 3729 cm^{-1}, 80 ~ 250 ^oC at 3732 cm^{-1} and 150 ~ 350 ^oC at 3745 cm^{-1}. Next, this happens on Si-OH-Al at 350 ~ 450 ^oC. Besides, on extra framework Al-OH species, it is 80 ~ 150 ^oC at 3781 cm^{-1}.

Table S3. peak assignments used in the NH_3-IR

IR features (cm^{-1})	Assignments
3782, 3778	Extra framework Al-OH
3745	Terminal Si-OH
3732, 3729	Internal Si-OH
3606, 3603	Bridged Al–(OH)–Si Brønsted groups
3347, 3286	NH_4^+ species
3338, 3293	NH_3 species
3392	NH_2 groups
3311	Na^+-NH_3 species
3199	Fe^{n+}-NH_3 species
1621, 1315	σ^{as} (NH_3) on Lewis acid sites
1503, 1463, 1429	σ^{as} (NH_4^+) on Brønsted acid sites

10. The difference in silanol species between HB-F and HDB-F

In order to clarify the drop of acid amount after dealumination for HB-F, the ex-FTIR was carried out on HB-F and HDB-F, shown in Figure S8. The peaks at 3780, 3742, 3732, 3729 and 3602 cm^{-1} are shown in Table S3. The signal of 3545 cm^{-1} is attributed to the hydrogen bonding silanol species. After dealumination, a large amount of internal silanol species appears and further transforms into the hydrogen bonding silanol species [4]. Thus, the internal silanol species (3732/3729 cm^{-1}) reduced obviously. Besides, most of extra-framework and Al-OH (3780 cm^{-1}) and part of Si-OH-Al (3602 cm^{-1}) are also removed. Correspondingly, the signal of 3545 cm^{-1} increases significantly.

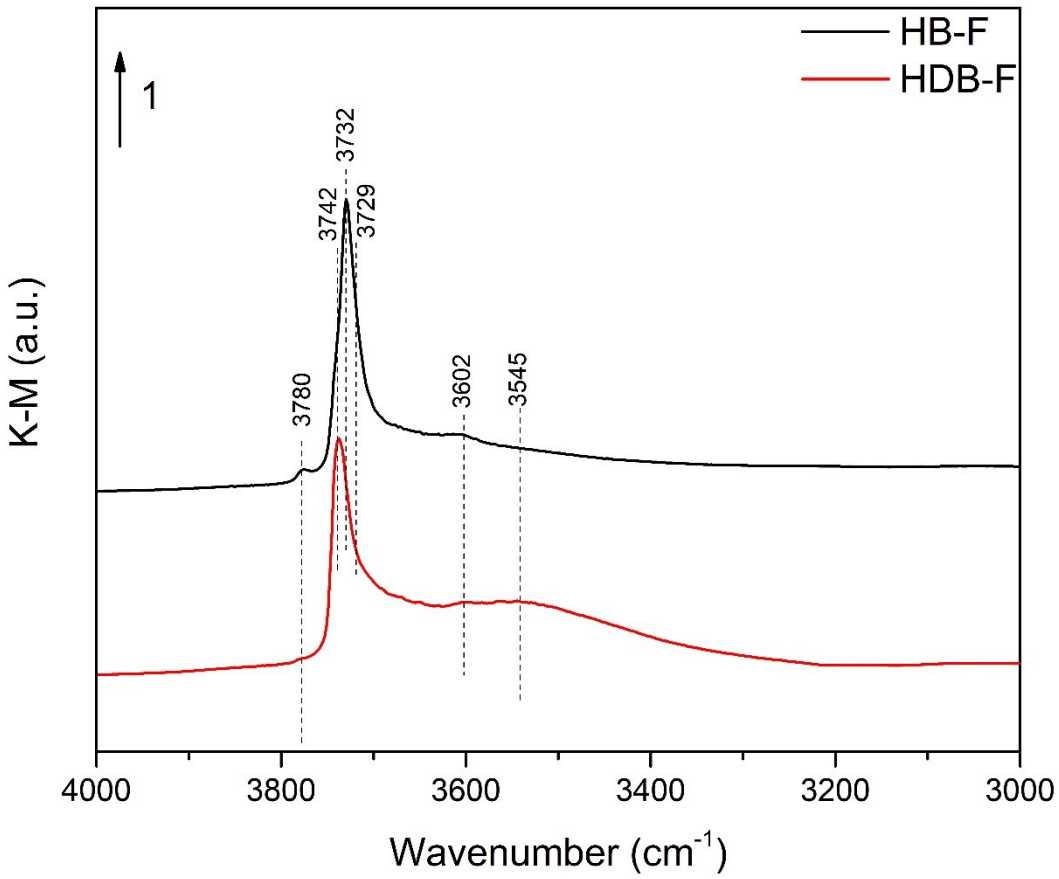

Figure S8. The ex-FTIR spectra of HB-F and HDB-F at 4000 ~ 3000 cm^{-1}.

11. The results of NO_x adsorption capacity

Table S4 shows the NO_x adsorption capacity by the value of NO_x adsorption/ total Pd content and the value NO_x adsorption per gram sample.

Table S4 The NO_x adsorption capacity of Pd/beta samples and Pd/beta-t samples.

Pd/beta samples	NO_x adsorption capacity (umol/g_{cat})	NO_x adsorption capacity / total Pd content	Pd/beta-t samples	NO_x adsorption capacity (umol/g_{cat})	NO_x adsorption capacity / total Pd content
PB-F	67.9	0.72	PB-F-t	29.1	0.31
PB-750	65.5	0.70	PB-750-t	18.4	0.20
PB-800	68.3	0.73	PB-800-t	15.4	0.16
PB-850	35.1	0.37	PB-850-t	10.7	0.11
PDB-F	24.7	0.26	PDB-F-t	19.6	0.21
PDB-750	26.0	0.28	PDB-750-t	19.2	0.20
PDB-800	30.6	0.33	PDB-800-t	20.3	0.22
PDB-850	22.2	0.24	PDB-850-t	14.1	0.15

Reference

1. Naccache, C., M. Primet, and M.V. Mathieu, *Study of Hydrogen and Carbon Monoxide Interactions with Palladium-Y Zeolite by ESR and IR Spectroscopy.* Advan. Chem. Ser., 1973. **121**: p. 266-280.
2. Wang, L., et al., *Role of Bronsted acidity in NH3 selective catalytic reduction reaction on Cu/SAPO-34 catalysts.* Journal of Catalysis, 2015. **324**: p. 98-106.
3. Baran, R., et al., *Influence of the nitric acid treatment on Al removal, framework composition and acidity of BEA zeolite investigated by XRD, FTIR and NMR.* Microporous and Mesoporous Materials, 2012. **163**: p. 122-130.
4. Maier, S.M., A. Jentys, and J.A. Lercher, *Steaming of Zeolite BEA and Its Effect on Acidity: A Comparative NMR and IR Spectroscopic Study.* The Journal of Physical Chemistry C, 2011. **115**(16): p. 8005-8013.
5. Vimont, A., F. Thibault-Starzyk, and J.C. Lavalley, *Infrared spectroscopic study of the acidobasic properties of beta zeolite.* Journal of Physical Chemistry B, 2000. **104**(2): p. 286-291.